Cationic (η^5-C_5Me_4R)Rh(III) Complexes with Metalated Aryl Phosphines Featuring η^4-Phosphorus-plus-Pseudoallylic Coordination

María F. Espada, Ana C. Esqueda,[†] Jesús Campos, Miguel Rubio, Joaquín López-Serrano, Eleuterio Álvarez, Celia Maya and Ernesto Carmona*

Instituto de Investigaciones Químicas (IIQ) and Departamento de Química Inorgánica, CSIC and Universidad de Sevilla, Avda. Américo Vespucio 49, 41092 Sevilla, Spain

[†]Escuela de Nivel Medio Superior de León, Universidad de Guanajuato. Hermanos Aldama y Blvd. Torres Landa s/n. León, Gto. México. CP 37480.

Email: guzman@us.es

ABSTRACT: In this contribution we study experimentally and computationally some electrophilic cationic (η^5-C_5Me_4R)Rh(III) complexes containing a cyclometalated bis(aryl)phosphine, PR'Ar_2. The phosphine Ar groups feature methyl substituents at the 2- and 6-positions of the aromatic rings allowing the formation of complexes [(η^5-C_5Me_4R)Rh(C^P)]$^+$ (**3**$^+$), where the metalated phosphine exhibits η^4 coordination to rhodium through phosphorus and the carbon atoms of the adjoining pseudoallylic functionality. The solution and solid-state structure of complexes **3**$^+$ has been studied by NMR and X-ray methods, and their electronic properties investigated with the aid of DFT calculations. The Lewis acid behavior of complexes **3**$^+$ has also been addressed, concentrating on reactivity toward CO, H_2 and hydrosilanes. Some catalytic Si-H/Si-D exchange and hydrosilylation reactions are also reported.

INTRODUCTION

Complexes of Rh(III) and Ir(III) built on a (η^5-C_5Me_5)M framework are the subject of numerous experimental and computational studies, owing to their capacity to participate in a plethora of chemical transformations, comprising many catalytic reactions.[1,2] In recent years we have investigated diverse complexes of this type, particularly those that possess a monoanionic cyclometalated phosphine ligand, C^P. It has long been known that the cyclometalation reaction is considerably facilitated by steric hindrance and by the formation of a stable five-member ring.[3] Accordingly, we chose aryl phosphines fulfilling these requirements, principally some mono- and bis-xylyl phosphines, PR_2Xyl and $PRXyl_2$, where R is an alkyl group and Xyl stands for 2,6-$Me_2C_6H_3$. Other closely related $PRAr_2$ phosphines were also studied.[4-7]

With the existing information on the interesting reactivity reported for the parent [(η^5-C_5Me_5)M(Me)(PMe_3)($ClCH_2Cl$)]$^+$ (M = Ir, Rh) complexes,[8] particularly in C—H bond activation reactions, the initial objective of this work was to ascertain whether the related metalacyclic complexes [(η^5-C_5Me_5)M(C^P)($ClCH_2Cl$)]$^+$, incorporating the M—C σ bond and the P-donor atom within the chelating C^P ligand, would behave similarly. None of the new compounds prepared was reactive under mild conditions toward intermolecular C—H bond activation, although those derived from the $PMeXyl_2$ ligand, exhibited interesting dynamic and chemical behavior. Instead of the foreseen CH_2Cl_2 adducts, both the rhodium[4] and the iridium[5a,6] complexes of this ligand featured a metalated phosphine with an unusual η^4-coordination involving the phosphorus atom and the contiguous pseudoallylic fragment. This un-

common structural motif is thought to be responsible for their unusual reactivity properties, including intermolecular H—H and Si—H activation,[4] as well as intramolecular C—H oxidative cleavage and C—C bond formation.[5a]

The formally tridentate, η^4-coordination mode of the metalated $PMeXyl_2$ ligand could only be authenticated by X-ray crystallography for one rhodium complex, and was preliminary communicated along with highly efficient catalytic hydrogen isotope exchanges in a variety of hydrosilanes (Si—H, Si—D and Si—T).[4] The same type of ligand coordination was unequivocally established by NMR methods in some related iridium complexes, but could not be substantiated by X-ray studies, as single crystals could not be grown.[5a,6] Moreover, although this coordination cannot be viewed as exceptional, for after all it combines P- and η^3-benzylic bonding, surprisingly it finds no precedent among the compounds registered in the Cambridge Structural Database (CSD).[9] It is additionally puzzling that such a structure appears not to be accessible for closely related Rh and Ir complexes of the mono(xylyl) phosphines PR_2Xyl (R = Me, Ph, ^{i}Pr, Cy).[7] For rhodium, stable CH_2Cl_2 adducts $[(\eta^5\text{-}C_5Me_5)Rh(C\text{^}P)(ClCH_2Cl)]^+$ derived from PMe_2Xyl and P^iPr_2Xyl were observed, whereas iridium yielded similar adducts when coordinated to the less bulky phosphines PMe_2Xyl and PPh_2Xyl, and hydride-alkylidene complexes resulting from α—H elimination when the bulkier P^iPr_2Xyl and PCy_2Xyl were utilized.[7]

Considering the above, we pursued additional work on the occurrence and stability of the η^4, P-plus-pseudoallylic cyclometalated structure. Herein we report experimental and computational studies on a variety of $(\eta^5\text{-}C_5Me_5R)Rh(III)$ complexes of metalated $PR'Ar_2$ ligands (R' = Me, Et; Ar = aryl group, *vide infra*). The structure of the chloride precursors is schematically represented in Figure 1. We focus attention on the rhodium-cyclometalated phosphine linkage exhibiting η^4-coordination and discuss its solution dynamic behavior, X-ray metrical parameters and reactivity towards H_2, silanes and catalytic hydrosilylation. Computational studies are also provided. As noted briefly, part of this work has been communicated.[4,10]

RESULTS AND DISCUSSION

Neutral hydride and chloride complexes. To gain access to the target cationic complexes $[(\eta^5\text{-}C_5Me_4R)Rh(C\text{^}P)]^+$ containing a cyclometalated $PR'Ar_2$ phosphine, the corresponding neutral chloride precursors were needed (Figure 1)

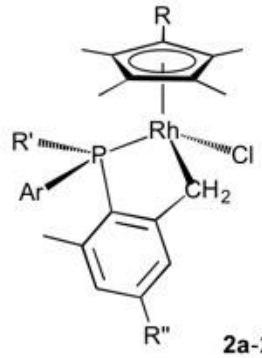

2a-2g

R = R' = Me; R" = H, **a**; Me, **b**; OMe, **c**; F, **d**

R = Me, R' = Et, R" = H, **e**

R = Bu^t, R' = Me, R" = H, **f**; R = $Ar^{Bu^t_2}$, R' = Me, R" = H, **g**

R = $SiMe_3$, R' = Me, R" = H, **i**

Figure 1. Rh(III) chloride complexes **2**, utilized in this work and labeling scheme. As indicated in the text $Ar^{Bu^t_2}$ represents 3,5-Bu^t_2-C_6H_3.

While comparable iridium complexes were readily prepared from the iridium dimer $[(\eta^5\text{-}C_5Me_5)IrCl_2]_2$ and the corresponding $PRAr_2$ phosphine under appropriate experimental conditions,[5,6] for rhodium the analogous reaction proved unsatisfactory, and gave rise to a manifold of products containing only low yields of the desired complex. Accordingly, complexes **2a**-**2g** were obtained by a somewhat more elaborated procedure that yielded first the related hydrides **1a**-**1g** accompanied by small amounts of the desired chlorides. The hydrides formed in a two-step reaction of $[RhCl(C_2H_4)_2]_2$, first with the phosphine at -40 ºC and then with $Zn(C_5Me_5)_2$ as cyclopentadienyl transfer reagent.[11] The resulting mixture was stirred for about 5h allowing to warm at -20 ºC, and then worked up at room temperature. Direct cyclometalation was observed with formation of hydrides **1a**-**1g**, along with minor amounts of chlorides **2a**-**2g**, the formation of the latter being a consequence of the high reactivity of the hydrides toward chlorinating agents. Indeed, addition of CH_2Cl_2 or $CHCl_3$ to the crude reaction mixtures produced exclusively the chloride complexes **2a**-**2g**, that were isolated in high yields (≥ 80%). Scheme 1 outlines the synthesis of **2e**, derived from the phosphine $PEtXyl_2$.

Scheme 1. Synthesis of chloride complex 2e.

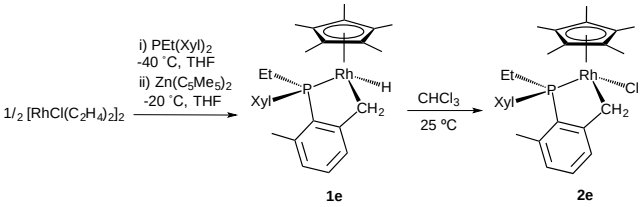

No attempts were made to fully characterize hydride complexes **1a**-**1g** because they were considered of secondary importance for the objectives of this work. Nevertheless, their characteristic NMR signals were unambiguously identified in mixtures with the corresponding chlorides. Furthermore, complex **1a** was synthesized independently from the reaction of **2a** with $NaBH_4$, although due to its marked reactivity toward oxygen and chlorinated solvents, analytically pure samples could not be obtained (see the Experimental Section for details). We, however, managed to isolate microanalytically pure samples of the hydride complex **1i** derived from $PMeXyl_2$ but containing $C_5Me_4SiMe_3$ as the capping ligand and provide full characterization data in the accompanying SI. All of the chloride complexes **2a**-**2g** were obtained as a single diastereoisomer with the stereochemistry shown in Scheme 1 for **2e**, with the only exception of **2c** that formed as a 3:2 mixture of stereomers. The compounds **2a**-**2g** were fully characterized by microanalysis and NMR spectroscopy. A comprehensive set of NMR data can be found in the SI. In addition, the solid-state molecular structures of compounds **2a**, **2b** and **2g** were determined by single-crystal X-ray studies. Figures S2 and S3 collect ORTEP perspective views of the molecular structures of complexes **2b** and **2g**, respectively. The structure of **2a** is shown in Figure 2 (left) to facilitate comparison with that of the corresponding cationic complex $\mathbf{3a}^+$ (*vide infra*).

Cationic complexes resulting from chloride abstraction from compounds 2. Reactions of the cyclometalated chloride complexes **2** with $NaBAr_F$ (BAr_F = $B(3,5\text{-}C_6H_3(CF_3)_2)_4$) in the presence of a Lewis base L, gave the expected cationic adducts $[(\eta^5\text{-}C_5Me_5)Rh(C\text{^}P)(L)]^+$, ($\mathbf{3{\cdot}L}^+$), that were isolated as salts of the BAr_F anion. In general, compounds $\mathbf{3{\cdot}L}^+$ formed as a mixture of *syn* and *anti* diastereomers, with the former being predominant. Carbonyl adducts $\mathbf{3{\cdot}CO}^+$ were generated from all complexes **2** except **2g**. For the $C_5Me_4Bu^t$ system the acetonitrile derivative $\mathbf{3f{\cdot}NCMe}^+$ was also isolated (Scheme 2), while from the parent compound **2a**, $\mathbf{3{\cdot}L}^+$ cations were also obtained for L = NCMe, NH_3, PMe_3,

CNXyl and C_2H_4. Here we concentrate our attention on the carbonyl complexes **3a·CO$^+$**-**3f·CO$^+$**, characterization data for other **3·L$^+$** compounds are given in the SI. Some of these adducts, viz. **3a·CO$^+$**, **3a·NCMe$^+$** and **3a·C$_2$H$_4^+$** were additionally studied by X-ray crystallography (see below and also SI).

Scheme 2. Synthesis of the cationic adducts 3f·CO$^+$ and 3f·NCMe$^+$.

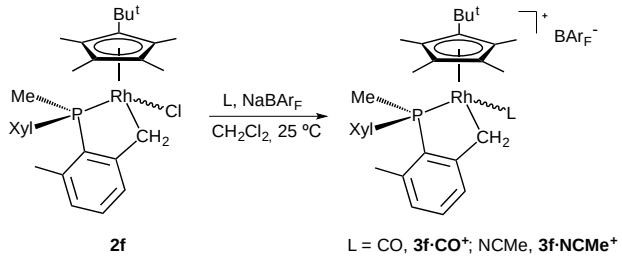

Carbonyl complexes **[3·CO][BAr$_F$]**, were obtained as yellow or orange solids. In the $^{13}C\{^1H\}$ NMR spectra, the carbonyl ligand resonates at around 189 ppm as a doublet of doublets, with $^1J_{CRh} \approx 75$ and $^2J_{CP} \approx 20$ Hz. The IR spectra display the expected carbonyl stretching vibration in the short interval 2055-2050 cm^{-1}, except for the F-substituted complex **3d·CO$^+$**, where it is slightly shifted to higher wavenumbers (2060 cm^{-1}). The high ν(CO) values hint back donation of of somewhat smaller magnitude than in the Ir(III) analogues,[12] which feature bands at 2030-2035 cm^{-1} (2040 cm^{-1} in the fluoro-substituted counterpart of **3d·CO$^+$**). This electronic picture is common for cationic carbonyl complexes of the transition metals,[13] including other late transition metals like Pt(II) and Au(I). Also in accordance with these arguments, **3a·CNXyl$^+$** exhibits the ν(C≡N) band at 2150 cm^{-1}, which is approximately 35 cm^{-1} higher in energy than in the free CNXyl. Clearly, the cationic Rh(III) center of the [(η^5-C$_5$Me$_5$)Rh(C^P)]$^+$ fragments investigated has weak capability to act as π-donor toward π-acid ligands, and moreover, the electronic properties do not change notably with the constitutional modifications that were introduced in the cyclopentadienyl and phosphine ligands employed in this work.

Scheme 3. Synthesis of cationic complex 3d$^+$ as a representative example of cyclometalated phosphine with η^3-benzylic coordination.

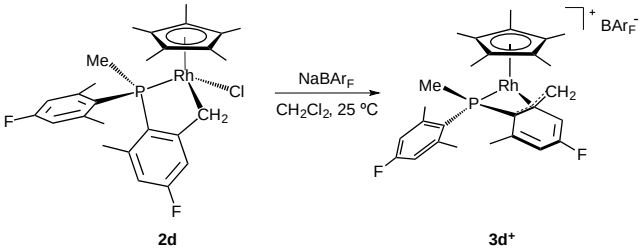

In contrast to previous results for the related rhodium and iridium complexes [(η^5-C$_5$Me$_5$)M(Me)Cl(PMe$_3$)],[8] CH_2Cl_2 solutions of the chlorides **2** reacted at room temperature with NaBAr$_F$ (or AgPF$_6$) to afford solvent-free cationic complexes [(η^5-C$_5$Me$_5$)Rh(C^P)]$^+$, (**3$^+$**), in which the cyclometalated phosphine is bonded to rhodium in an η^4 fashion, through the phosphorus and the three carbon atoms of the adjoining benzylic fragment (Scheme 3). Low-temperature $^{31}P\{^1H\}$ NMR monitoring of this reaction (**2a**, CD_2Cl_2, -80 ºC to room temperature) revealed that at -80 ºC complex **3a$^+$** was the major solution species, though accompanied by minor amounts of another product responsible for a doublet resonance at 48.3 ppm ($^1J_{PRh}$ = 160 Hz). The latter is probably due to the expected[8] adduct **3a·CH$_2$Cl$_2^+$** (*vide infra*) that converted into the pseudoallylic species **3a$^+$** above -30 ºC. Since as explained above effecting the reactions in the presence of NCMe furnished adducts **3·NCMe$^+$**, it is evident that the weakly coordinating CH_2Cl_2 is unable to change the coordination of the benzylic terminus from

η^3 to η^1. It is also apparent that an equilibrium is established between complexes $\mathbf{3}^+$ and $\mathbf{3{\cdot}L}^+$ (Scheme 4). The former feature a characteristic $^{31}P\{^1H\}$ NMR resonance in the vicinity of -15 ppm (-4.4 ppm for the $PEtXyl_2$-derived complex $\mathbf{3e}^+$), whereas the latter resonate at markedly higher frequencies (near 40 ppm; for $\mathbf{3e{\cdot}CO}^+$ at 54.2 ppm). Thus, equilibria alike that represented in Scheme 4 can be readily analysed by $^{31}P\{^1H\}$ NMR spectroscopy. Poor σ donors like NCMe, MeOH, EtOH and $Me_2C(O)$ (neat solvents) formed adducts $\mathbf{3{\cdot}L}^+$ of fleeting existence, identifiable by resonances in the region *ca.* 38-50 ppm that reverted to the corresponding base-free cations $\mathbf{3}^+$ upon solvent removal by action of vacuum. Predictably, stronger donors (CO, CNXyl, NH_3, PMe_3) originated stable $\mathbf{3{\cdot}L}^+$ adducts, while $\mathbf{3a{\cdot}C_2H_4}^+$ was found to be stable as a solid although it lost readily C_2H_4 in solution.

Scheme 4. Equilibria between complexes $\mathbf{3}^+$ and $\mathbf{3{\cdot}L}^+$ in the presence of the Lewis base.

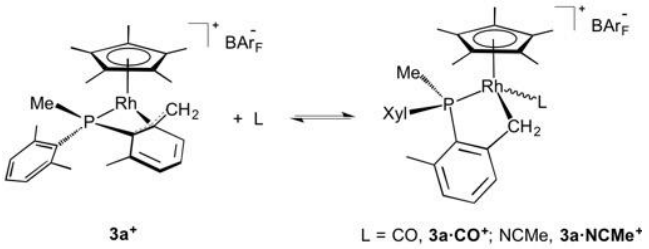

In contrast to homologous iridium compounds that, as briefly noted, could not be isolated as single crystals, samples of several rhodium complexes $\mathbf{3}^+$ suitable for X-ray studies were procured. Figure 2 depicts the molecular structures of complex $\mathbf{3a}^+$**,** while structural data for complexes $\mathbf{3d}^+$, $\mathbf{3e}^+$ and $\mathbf{3f}^+$can be found in the Supporting Information (Figure S4). For comparative purposes the structure of the neutral chloride **2a** has been included in Figure 2

Differences in the spatial distribution and metal coordination of the cyclometalated $PMeXyl_2$ moiety of complexes **2a** and $\mathbf{3a}^+$ are evident at first sight (Figure 3). In contrast to compound **2a**, where only the terminal P and C atoms of the chelating ligand are bound to rhodium, in $\mathbf{3a}^+$ the two aromatic ring carbon atoms of the benzylic unit are also metal-bonded giving rise to an η^3-benzylic end that complements P-binding. The aromatic ring that is part of the metalacyclic structure of **2a** forms an angle of *ca.* 64.4º with the η^5-C_5Me_5 ring, while the dihedral angle between the free Xyl substituent and the C_5Me_5 is of *ca.* 20.6º, and almost perpendicular to the other (~ 77.5º). Contrarily, the P and the benzylic carbon atoms of cation $\mathbf{3a}^+$ (P1, C17, C11 and C12) form an almost planar arrangement, practically parallel to the C_5Me_5 ring (dihedral angle 7.3º). Consequently, this distribution of the donor atoms leads to a mixed-sandwich structure, somehow related to that of the decamethylrhodocenium complex.[14] In fact, the mean Rh—C_{ring} distance in the latter complex of 2.180(5) Å is comparable to the Rh-C_5Me_4R mean distances found for complexes $\mathbf{3}^+$ (e.g. 2.194(5) in $\mathbf{3a}^+$). Although the Rh—P distances in complexes $\mathbf{3}^+$ are similar (2.257(1)-2.269(7) Å) and do not diverge significantly from those in compounds **2**, the two aromatic carbon atoms of the metalated moiety in complexes $\mathbf{3}^+$ approach to rhodium to well within bonding distances, somewhat less the adjacent carbon atom (C17 in Figure 3, 2.254(4) Å) but significantly more the central benzylic carbon (C12 in Figure 3) at 2.200(5) Å. The fluctuation experienced by the metalated unit upon conversion of **2** into $\mathbf{3}^+$ causes the free Xyl radical to dispose itself nearly perpendicular to the η^4-P, C, C', C'' and C_5Me_5 planes, pertinent angles in $\mathbf{3a}^+$ being 87.4 and 85.4º, respectively. As can be seen in Figures 3 and 4, one of the Me groups of the free Xyl ring (C26 in Fig. 3; C26, C28 and C30 for $\mathbf{3d}^+$, $\mathbf{3e}^+$ and $\mathbf{3f}^+$, respectively, in Fig. 4) and the corresponding *ipso* carbon atom, hover over the open space of the wedge created by the Rh—P and Rh—$C_{terminal}$ bonds within the η^4-(C^P) ligand. These Rh···Me contacts are far from bonding (*ca.* 3.876(5) Å for $\mathbf{3a}^+$), nevertheless the existence of this ring permits attainment of a kinetically facile equilibrium with a higher energy species $\mathbf{A}^+$ (see computational discussion next) that exhibits a δ CH_3⇀Rh agostic interaction[15] and κ^2-

coordination of the metalated xylyl ring. Despite lying largely on the side of complexes $\mathbf{3}^+$, this equilibrium appears to facilitate the observed η^4-phosphine structure and above all the H_2 and hydrosilane activation reactions (*vide infra*).

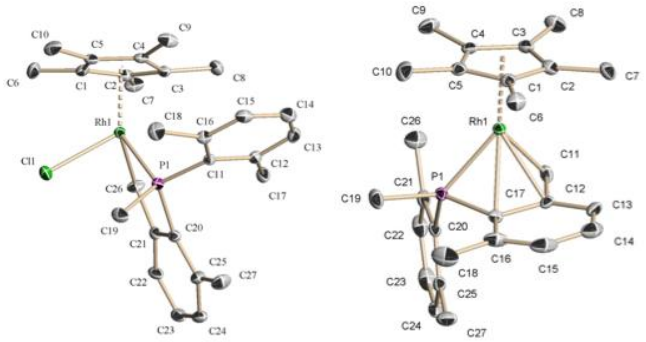

Figure 2. ORTEP perspective views of the molecules of **2a** and $\mathbf{3a}^+$; hydrogen atoms are excluded for clarity and thermal ellipsoids are set at 50%. Selected bond distances (Å) and angles (º) for **2a**: Rh1—P1 = 2.255(1); Rh1—C26 = 2.101(4); Rh1—Cl1 = 2.390(1); P1—C20 = 1.821(3); C26—C21 = 1.488(5); C20—C21 = 1.391(5); P1-Rh1-C26 = 81.5(1); Rh1-P1-C11 = 115.7(1); Cl1-Rh1-C26 = 87.9(1); Cl1-Rh1-P1 = 90.05(3). Selected bond distances (Å) and angles (º) for $\mathbf{3a}^+$: Rh1—P1 = 2.260(1); Rh1—C17 = 2.254(5); Rh1—C12 = 2.201(5); Rh1—C11 = 2.135(5); P1—C17 = 1.788(5); C17—C12 = 1.458(7); C12—C11 = 1.439(7); P1-C17-C12 = 111.8(4); C17-C12-C11 = 117.6(4).

Computational studies of the electronic structures of these complexes were undertaken. Analysis of the calculated electron density of $\mathbf{3a}^+$ (DFT-optimized geometry in the gas phase, see the computational details) was carried out within the Quantum Theory of Atoms in Molecules formalism.[16] Accordingly, three bond critical points (*bcp*) and bond paths connect the Rh1 and the P1, C17 and C12 atoms (no *bcp* was located between any of the hydrogen atoms on C26 and the rhodium atom; see Figure 4) and account for the linkage between the Rh atom and the cyclometalated phosphine. The Laplacian of the electron density ($\nabla^2\rho_b$) is positive at these points, which is diagnostic of *close shell* interactions. In addition, the values of the local Potential (V_b) and Kinetic (G_b) energies and their ratios ($1 < |V_b|/G_b < 2$) are consistent with metal-ligand interactions (Table 1).[17] Interestingly, DFT calculations located a second minimum for a species, $\mathbf{A}^+$ (Figures 3 and 4), 5 kcal·mol^{-1} less stable than $\mathbf{3a}^+$ ($\Delta\boldsymbol{E}$ in dichloromethane), which features κ*C*, κ*P* bidentate binding of the cyclometalated phosphine, as indicated by two *bcps* and bond paths connecting the rhodium and the P1 and C11 atoms (and the absence of *bcp*s between Rh1 and C12 or C17). The loss of the pseudoallylic interaction between Rh and the phosphine in $\mathbf{A}^+$ is partially offset by the establishment of a δ-agostic interaction[15] between the rhodium atom and one of the methyl substituents of the pendant xylyl group of the phosphine, which is demonstrated by a new *bcp* connecting Rh1 and one of the hydrogen atoms on C26 (Figure 3). The role of $\mathbf{A}^+$ in the reactivity of $\mathbf{3a}^+$ will be discussed below. Localized molecular orbital analysis (NBO)[18] of $\mathbf{3a}^+$ and $\mathbf{A}^+$ offers a complementary description of the bonding around the rhodium atom. In $\mathbf{3a}^+$, a donor-acceptor interaction is established between a π orbital localized on the C17 and C12 atoms and an empty d orbital of the rhodium atom. This interaction is absent in $\mathbf{A}^+$, but in turn the new δ-agostic interaction arises from a donor acceptor interaction between a σ C—H bond and an empty σ* Rh—C(Cp). Additional data on the AIM and NBO analyses can be found in the Supplementary Information (Figures S11-12 and Table S19).

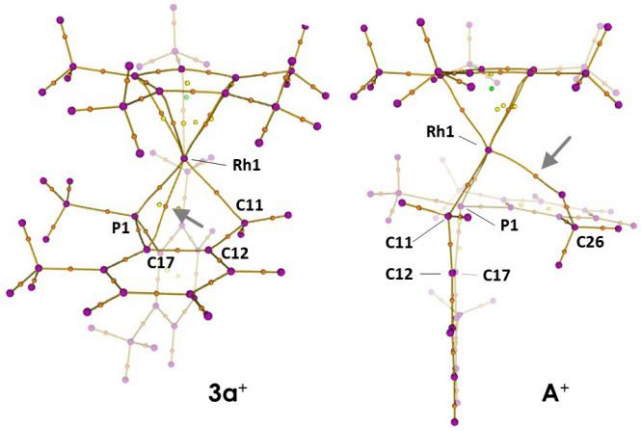

Figure 3. Molecular graph of complexes **3a**$^+$ (left) and **A**$^+$ (right) showing bond critical points (*bcp*) and bond paths connecting the rhodium atom and the cyclometalated phosphine. Relevant bcps and bond paths are highlighted with arrows.

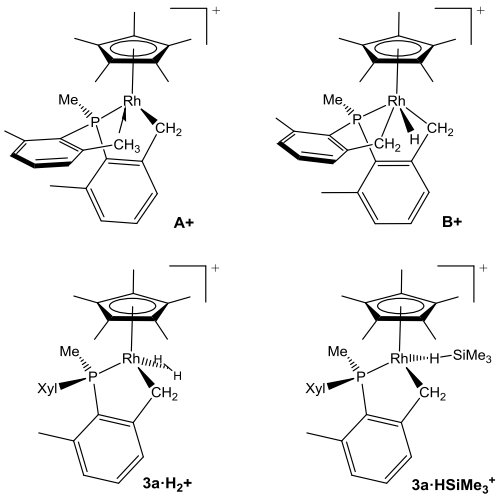

Figure 4. Structural representation for some relevant computed intermediates.

Table 1. Selected data of from the electron density of 3a$^+$ and A$^+$ at relevant bond critical points of the Rh linkage.

	bcp connecting atoms	ρ^a	$G_b{}^b$	$V_b{}^b$	$\nabla^2\rho^c$
3a$^+$	Rh1—P1	0.0910	0.0661	-0.0977	0.1383
	Rh1—C17	0.0692	0.0634	-0.0778	0.1962
	Rh1—C11	0.0961	0.0734	-0.1039	0.1714
A$^+$	Rh1—P1	0.0973	0.0670	-0.1012	0.1314
	Rh1—C11	0.1047	0.0674	-0.1036	0.1242
	C26—H ⇀ Rh	0.0485	0.0543	-0.0589	0.1986

[a]e·bohr^{-3}, [b]hartree, [c]e·bohr^{-5}

NMR data for complexes **3**$^+$ are in full agreement with the solid state structure presented in the preceding paragraphs and highlight in addition an interesting dynamic behavior. Using as a reference the parent complex **3a**$^+$, the $^{31}P\{^1H\}$ NMR spectrum contains a shielded doublet at -14.7 ppm ($^1J_{PRh}$ = 138 Hz). The ^1H NMR spectrum features methyl resonances at 1.74 ($C_5\mathit{Me}_5$, d, $^4J_{HP}$ = 2.5 Hz), 2.66, 2.59 and 2.12 ppm, the latter three appearing as singlets and being attributable to the xylyl group substituents

(Me_α, Me_β and Me_γ in Figure 5). The Rh—CH_2 protons of the pseudoallyl moiety resonate with quite different chemical shifts, specifically 3.06 (H_α) and 1.34 (H_β). The former appears as a doublet of triplets ($^2J_{HH}$ = 4.5, $^2J_{HRh}$ = $^3J_{HP}$ = 1.5 Hz) and the latter as a doublet of doublets ($^2J_{HRh}$ = 1.5, $^3J_{HP}$ = 10.0 Hz). The associated ^{13}C signal is a doublet of doublets centered at 42.1 ppm ($^1J_{CRh}$ = 15, $^2J_{CP}$ = 2 Hz) and exhibits a one-bond ^{13}C-^{1}H coupling constant of 160 Hz). It is also pertinent to mention that the aromatic carbon atoms participating in the η^3-benzylic interaction (C1 and C2 in Fig. S1, see the SI) are considerably shielded in comparison with the corresponding signals in the free Xyl substituent, for they resonate at 104.3 and 77.6 ppm, respectively (see Fig. S1) while, for instance, the *ipso* carbon atom C5 appears at 120.8 ppm (vs. the 77.6 ppm value found for C2).

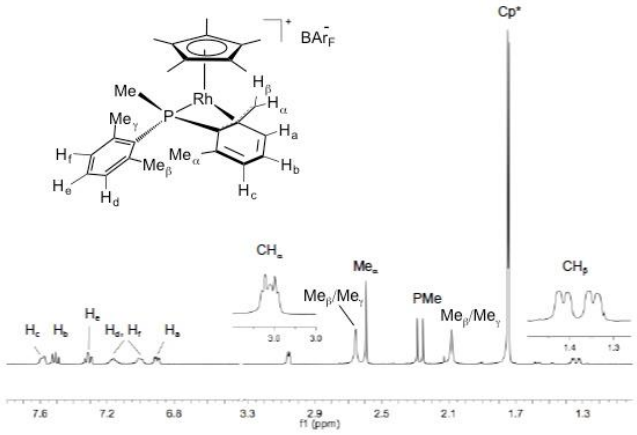

Figure 5. ^{1}H NMR spectrum of complex **3a**$^+$ and labelling scheme for complex **3a**$^+$ utilized for assignment of ^{1}H and ^{13}C NMR signals.

The ^{1}H NMR spectrum of **3a**$^+$ contains several broad signals that denote solution dynamic behavior. Variable temperature NMR studies (10 to 75 ºC) revealed that in addition to rotation of the free Xyl ring around the P—C bond exchanging Me_β and Me_γ in Figure 5, the metalated and the non-coordinated xylyl units commute their roles, that is upon metalation of the latter the former becomes disengaged. This dynamic behavior is similar to that disclosed for an iridium complex analogue.[5a] 2D EXSY NMR experiments performed in the interval 25-45 ºC showed transfer of magnetization between the methyl groups Me_β and Me_γ of the non-metalated ring, as well as between those and Me_α and Rh-CH_2 groups, although at a slower rate. We were able to determine the first-order rate constant for both exchange processes as 2.1 and 1.2 x 10^{-2} s^{-1}, corresponding to $\Delta \boldsymbol{G}_{298K}^{\ddagger}$ of 18 and 21 kcal mol^{-1}, respectively. These barriers are significantly higher than those measured for the iridium counterpart ($\Delta \boldsymbol{G}^{\ddagger}$ = 13 and 17.3 kcal·mol^{-1}, respectively),[5a] in accordance with an exchange implicating, in both cases, a doubly metalated Rh(V) hydride intermediate.[19]

Rather surprisingly, DFT calculations predict that rotation of the non-metalated Xyl ring of **3a**$^+$ has a barrier that exceeds 40 kcal·mol^{-1}. This result can be reconciled with the experimental data if it is assumed that **3a**$^+$ is in equilibrium with the aforementioned intermediate **A**$^+$ ($\Delta \boldsymbol{E}$ = 5 kcal·mol^{-1}). The necessary coordination change of the cyclometalated phosphine from η^4 to the more common κ*C*, κ*P* bidentate binding has a barrier ($\Delta \boldsymbol{E}^{\ddagger}$ in dichloromethane) of 11.8 kcal·mol^{-1} (Figure 6). In the analogous iridium system,[5a] both the barrier and relative energy are significantly lower (6.4 and 0.9 kcal·mol^{-1}, respectively). Now, rotation of the Xyl ring has an energy barrier (See Figure S14 in the SI) of ca. 10 kcal·mol^{-1} from **A**$^+$, 15 kcal·mol^{-1} overall from **3a**$^+$, which is in good agreement with the experiments. Calculations also reveal that a higher energy (23.8 kcal·mol^{-1}) Rh(V) intermediate **B**$^+$ resulting from oxidative cleavage of the agostic C—H ⇀ Rh bond (Figures 4 and 6) makes possible the exchange of the two fragments after a barrier of 25.5 kcal·mol^{-1} is overcome, once again the barrier being significantly higher than for iridium (17.3 kcal·mol^{-1}).[5a] These results are in agreement with the lower accessi-

bility of the M(V) oxidation state for rhodium, although some stable Rh(V) complexes are known.[19] Recently, an unusual Rh(IV) coordination compound was reported by Crabtree and coworkers.[20] The computed energy barrier is in good agreement with the NMR measurements described above.

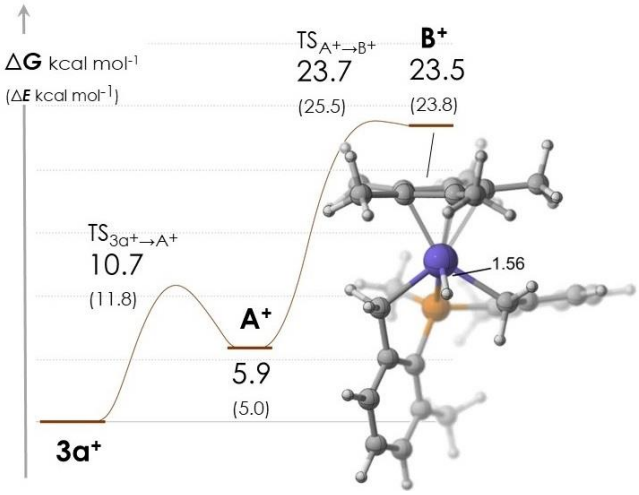

Figure 6. Calculated energy profile accounting for the dynamic behavior of **3a**$^+$ in solution and DFT-optimized geometry of the Rh(V) intermediate **B**$^+$. Gibbs energy and potential energy (in parentheses) data are in kcal·mol^{-1}.

Reactions of complexes 3a$^+$-3e$^+$ with dihydrogen and hydrosilanes. Catalytic C-H/C-D and Si-H/Si-D exchanges and hydrosilylation reactions. Studying the reactivity of the η^4-complexes **3**$^+$ toward dihydrogen and hydrosilanes, as substrates that possess only σ-bonding electrons, was an attractive target.[21] The iridium complex analogous to **3a**$^+$ was found to react with H_2 under ambient conditions with quantitative formation of a bis(hydride)Ir(V) species. The reaction was, however, reversible, H_2 removal under vacuum yielding back the starting Ir(III) derivative.[5a] In contrast to this observation, no reaction was detected when complexes **3a**$^+$-**3e**$^+$ were stirred at room temperature under 1 bar of H_2. Nevertheless, as briefly reported for **3a**$^+$,[4] upon cooling at -90 ºC minor quantities of a new cationic complex **4a**$^+$, in equilibrium with **3a**$^+$, were detected by NMR spectroscopy (Scheme 5). All complexes **3**$^+$ studied behaved similarly except the OMe substituted **3c**$^+$ (see Fig. 1) for which no observable product was detected. The new complexes **4**$^+$ were identified as cationic Rh(III) hydrides featuring a δ-agostic interaction[15] involving one of the Me substituents of the phosphine aryl rings. Although comprehensive NMR data for cations **4**$^+$ are provided in the SI, it is pertinent to mention that they exhibit a $^{31}P\{^1H\}$ doublet resonance notably shifted to higher frequencies (δ 27-30, $^1J_{PRh} \approx 140$ Hz), as well as two shielded ^1H resonances located at around -10 and 0 ppm, that undergo mutual exchange. The more shielded of the two, though broad, becomes sufficiently resolved as a doublet of doublets, with $^1J_{HRh}$ = 18.5 and $^2J_{HP}$ = 37 Hz, and has a spin-lattice relaxation time T_1 = 300 ms (data for **4a**$^+$), clearly corresponding to a Rh—H bond.[21] The exchanging, also broad, singlet in the proximity of 0 ppm has relative intensity corresponding to 3H atoms and is assigned to Rh⌐H_3C- agostic interaction.[15] The exchange process likely occurs by oxidative cleavage of the agostic C—H bond, as shall be described below.

Scheme 5. Reaction of complexes 3a$^+$, 3b$^+$, 3d$^+$ and 3e$^+$ with H_2.

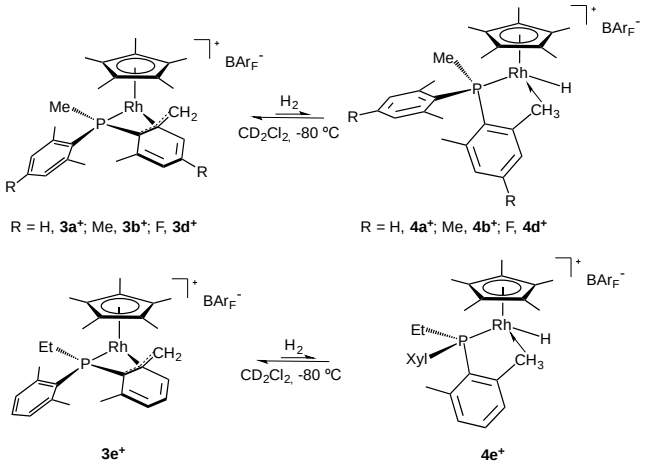

R = H, **3a**$^+$; Me, **3b**$^+$; F, **3d**$^+$ R = H, **4a**$^+$; Me, **4b**$^+$; F, **4d**$^+$

3e$^+$ **4e**$^+$

A final comment in regard with the H_2-promoted equilibria of Scheme 5 pertains to the relative stabilities of complexes **3**$^+$ and **4**$^+$. As briefly noticed, the putative agostic hydride **4c**$^+$ of the OMe substituted aryl phosphine could not be detected. Changing the *para* OMe substituent by a methyl group led to a **4b**$^+$:**3b**$^+$ ratio of roughly 2:98, whereas $PMeXyl_2$ (i.e. H at the 4-position of the rings) and the F-containing $PMeAr_2$ phosphine gave rise to improved **4a**$^+$:**3a**$^+$ and **4d**$^+$:**3d**$^+$ ratios of 10:90 and 17:83, respectively. For the $PEtXyl_2$ derivatives **4e**$^+$ and **3e**$^+$, the observed ratio was *ca.* 5:95. Although the differences are relatively small, they correlate with the ν(CO) changes discussed earlier for the carbonyl complexes **3·CO**$^+$, and reveal that the relative stability of the cationic agostic hydride complexes increases in the order OMe < Me < H < F, that is, with a decrease in the overall donor capacity of the $PMeAr_2$ phosphine utilized, and concomitant increase in the Lewis acidity of the 16-electron cationic Rh(III) center.

No apparent reactions were observed either when the above complexes **3**$^+$ were treated with $SiEt_3H$ and other hydrosilanes. Although reactivity similar to that represented in Scheme 5 for H_2 was reasonably expected, cationic agostic silyl complexes analogous to hydrides **4**$^+$ did not form in detectable concentrations. DFT calculations on the reactions with H_2 and $SiMe_3H$ (used as a model silane) were developed and suggested, though, the key intermediacy of both σ-H_2 and $HSiMe_3$ complexes in the corresponding reactions (Figure 7). Thus, *syn* and *anti* diasteromers of **3a·H$_2$**$^+$ and **3a·HSiMe$_3$**$^+$ were located as minima in the potential energy surface, however their formation from **3a**$^+$ is endergonic in all cases. *Syn*-**3a·H$_2$**$^+$ **lies** 7.2 kcal·mol^{-1} above **3a**$^+$ + dihydrogen (Δ***G*** in dichloromethane) and can be described as an η^2-σ-H_2 complex. Similarly, *syn*-**3a·HSiMe$_3$**$^+$ lies 4.6 kcal·mol^{-1} above the separated fragments, but then it is best described as an η^1-silane complex ($d_{Rh\text{-}H}$ = 1.81 Å, $d_{Rh\text{-}Si}$ = 3.27 Å).[22] Rh(III) hydride **4a**$^+$ was also modelled as a relatively stable species, and is only 1.9 kcal·mol^{-1} above **3a**$^+$ + H_2 at 295 K, which agrees with **4**$^+$ cations being detected by NMR at low temperature. These species interconvert through an energy barrier of 8.1 kcal·mol^{-1} from **3a·H$_2$**$^+$. The corresponding transition state has Rh(V) character, as indicated by the Rh-H distance of 1.57 Å (Figure 7). Nevertheless, at variance with the related Ir system,[5a] no Rh(V) bis(hydride) intermediate was located in this case. **3a·HSiMe$_3$**$^+$ also interconverts with the corresponding agostic silyl complex **5a**$^+$ in an analogous manner. In this case, formation of **5a**$^+$ is endergonic by 6.2 kcal·mol^{-1}, which justifies that the related species were never detected experimentally. It should be emphasized that both of the reversible exchange processes that have just been described can place hydrogen atoms from the H_2 and silane molecules onto the phosphine ligand of the metal complex.

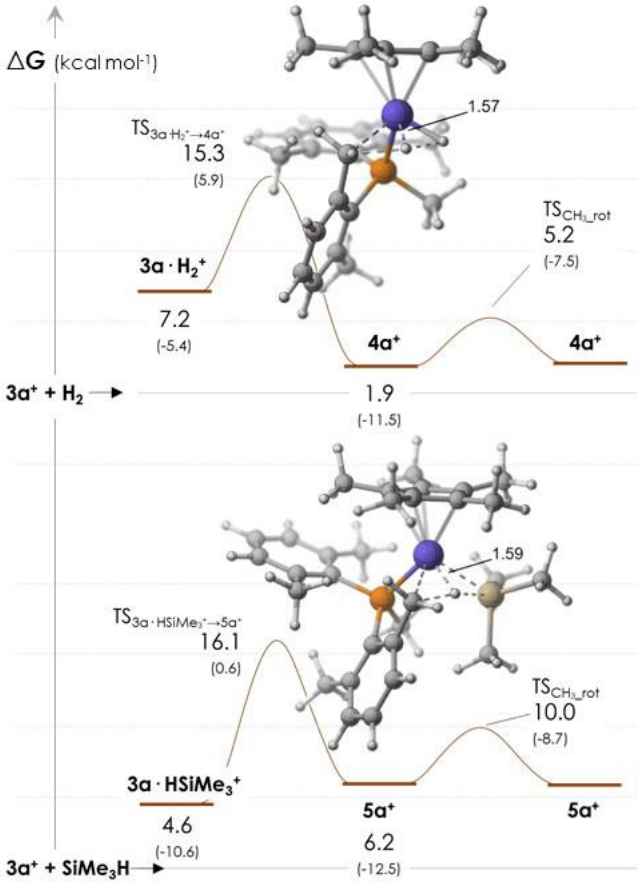

Figure 7. Calculated Δ***G*** profiles in dichloromethane (kcal·mol^{-1}) for the reactions of **3a**$^+$ with H_2 (upper trace) and Me_3SiH (lower trace). The first transition state in each profile (insets depict their DFT-optimized geometries) connects the σ-**3a**$^+$**·L** complex and the corresponding hydride and silyl cations **4a**$^+$ and **5a**$^+$. The second transition state corresponds to rotation of the Rh ← H_3C- methyl, which accounts for H/D exchange (see the SI for details). Data in parentheses are Δ***E*** in dichloromethane.

To complement the anterior computational findings, it should be mentioned that exposure of solutions of complexes **3a**$^+$-**3e**$^+$ to D_2 led to fast H/D exchange at all the benzylic CH_3 and metalated CH_2 sites. These observations allowed developing a catalytic synthesis of deuterated silanes[4] and its exploitation for several-gram-scale preparations of $SiEt_3D$, $SiMe_2PhD$ and $SiPh_2D_2$, using D_2 (0.5 bar) as the source of deuterium[10b] and the parent complex **3a**$^+$ as the catalyst in *ca.* 0.01 mol%. Tritiated silanes were also produced,[4] and since **3a**$^+$ catalyzed with high efficacy the hydrosilylation of carbonyl compounds[10a] and of the C≡N bonds of α,β-unsaturated nitriles,[10b] a highly convenient one-flask, two-step catalytic procedure for deutero- and tritiosilylation of the mentioned substrates was developed.[10]

Considering the similar chemical behavior of all complexes **3**$^+$, we have completed these studies with the investigation of the catalytic activity of complexes **3b**$^+$-**3e**$^+$ in related work involving D_2 and $SiEt_3H$ and $Si(SiMe_3)_3H$ as the silanes (Scheme 6). No significant differences were found among new complexes and the original catalyst **3a**$^+$, so that for instance quantitative Si-H/Si-D exchanges were disclosed for $SiEt_3H$ (≥ 99%) in CD_2Cl_2, at 50 ºC after 5 hours, under 0.5 bar of D_2, regardless of the nature of the original phosphine ligand. Similarly, conversion for $Si(SiMe_3)_3H$ was lower (*ca.* 30%) in all cases investigated. Reactions were performed at room temperature for 16 hours under otherwise analogous experimental conditions.

Scheme 6. Deuteration of hydrosilanes catalized by complexes 3b$^+$**-3e**$^+$**.**

A) $SiEt_3H$ —[Rh] (0.1 mol %), D_2 (0.5 bar), CD_2Cl_2→ $SiEt_3D$ + HD

B) $Si(SiMe_3)_3H$ —[Rh] (1 mol %), D_2 (0.5 bar), CD_2Cl_2→ $Si(SiMe_3)_3D$ + HD

In noticeable contrast with these results, the hydrosilylation[23,24] of the aromatic ketones ArC(O)Me (Ar = Ph, 1-naphtyl) was found to be markedly dependent on the phosphine substituents (Scheme 7 and Table 2). Thus, the *para*-methyl substituted precursor **3b**$^+$ had significantly diminished activity compared to **3a**$^+$, whereas both the *para*-methoxy analogue **3c**$^+$, and the $PEtXyl_2$ derivative **3e**$^+$ were inactive under similar conditions. Somewhat rewarding, the fluoro-containing complex **3d**$^+$ exhibited comparable if not superior activity than **3a**$^+$ (Table 2). To gain mechanistic insights, some additional experiments were performed.

Scheme 7. Hydrosilylation of aromatic ketones catalyzed by complexes 3b$^+$-3e$^+$.

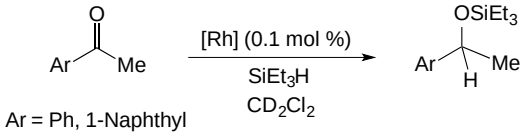

Table 2. Hydrosililation reaction.[a]

Entry	Catalyst	Ar	T (ºC)	t (h)	Conversion (%)
1	**3a**$^+$	Ph	25	14	≥ 99
2	**3b**$^+$	Ph	25	14	30
3	**3c**$^+$	Ph	25	14	0
4	**3d**$^+$	Ph	25	14	≥ 99
5	**3e**$^+$	Ph	25	14	0
6	**3a**$^+$	1-Naph	50	24	10
7	**3b**$^+$	1-Naph	50	24	0
8	**3c**$^+$	1-Naph	50	24	0
9	**3d**$^+$	1-Naph	50	24	15
10	**3e**$^+$	1-Naph	50	24	0

[a] Conditions: 0.1-0.5 mmol of substrate, 2.2 equiv of $SiEt_3H$; CD_2Cl_2 (0.5 mL).

In parallel tests, we monitored by low temperature $^{31}P\{^1H\}$ NMR spectroscopy (CD_2Cl_2, -80 ºC) the interaction of complex **3a**$^+$ with a hundredfold excess of $SiEt_3H$ and acetone. As anticipated, no reaction was detected for the silane while a 70:30 mixture of **3a**$^+$ and the corresponding acetone adduct, **3a·S**$^+$, was obtained in the second instance. Clearly, under our catalytic reaction conditions (Scheme 7), **3a**$^+$ is the catalyst resting state and is in equilibrium with lower concentrations of the ketone adduct. This is in dissimilarity with findings by Brookhart and coworkers on related hydrosilylation reactions catalyzed by

an also cationic Ir(III) pincer complex, where the catalyst resting state was a ketone adduct, in equilibrium with low concentrations of an η^1-σ-silane.[22,24b] An ionic mechanism implying R_3Si^+ transfer to the ketone to form an oxocarbenium ion $R_3SiOCR_2'^+$, subsequently reduced by a neutral Ir(III) dihydride was proposed, in close analogy with the ionic mechanism previously postulated by Piers when employing $B(C_6F_5)_3$ as the catalyst.[25]

Kinetic studies on the Ir(III) system also disclosed that the mechanism was zero-order in ketone and first-order in silane. Once more at variance with these observations, our Rh(III) catalytic reaction featured first-order dependence on both $SiEt_3H$ and the ketone (Figure 8). Besides, for acetophenone hydrosilylation a kinetic isotope effect (KIE) of k_H/k_D = 1.9 (± 0.1) was measured employing $SiEt_3H$ and $SiEt_3D$.

On the basis of these results and taking into consideration prior literature reports,[26,27] along with knowledge emanated from the experimental and computational studies already discussed, acetone hydrosilylation by $SiEt_3H$ could follow a variant of the Chalk-Harrod mechanism alike that presented in Scheme S1 (see the Supporting Information).

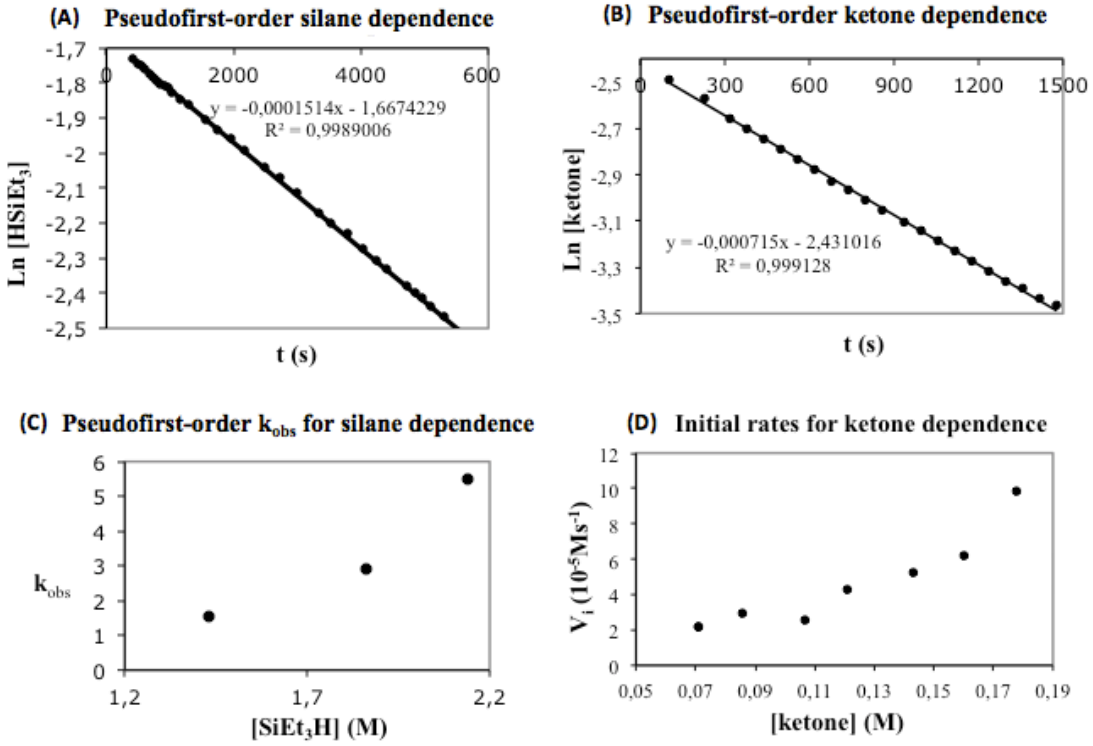

Figure 8. Kinetic studies for the reaction of acetophenone and triethylsilane at 25 ºC in CD_2Cl_2 catalyzed by 1^+. (A) Pseudofirst-order consumption of silane. Conditions: $[acetophenone]_o$ = 1.85M; $[HSiEt_3]_o$ = 0.18M; $[1^+]$ = 1.4x10^{-4}M. (B) Pseudofirst-order consumption of acetophenone. Conditions: $[acetophenone]_o$ = 0.09M; $[HSiEt_3]_o$ = 2.14M; $[1^+]$ = 1.4x10^{-4}M. (C) Plot of the observed rate constant, k_{obs}, of acetophenone consumption *vs* silane concentration (excess silane). (D) Plot of the initial rate, V_i, of acetophenone consumption *vs* ketone concentration (<10 % conversion, excess silane).

SUMMARY AND CONCLUSIONS

In summary, this work shows that cationic Rh(III) complexes of type $[(\eta^5\text{-}C_5Me_4R)Rh(C\text{^}P)]^+$, **3**$^+$, that contain a cyclometalated bis(aryl)phosphine PR'Ar_2, featuring 2,6-Me_2-substitution at the P-bonded

aryl groups, strongly favour η^4 coordination of the phosphine through the phosphorus atom and the adjacent metalated pseudoallylic unit. The η^4 structure is labile and is responsible for the facile intramolecular exchange between the metalated and the free phosphine Ar substituents, as well as for the interesting H—H and Si—H bond activation reactivity of the complexes. Changing the nature of the 4-substituent R'' of the $PMeAr_2$ phosphines (Ar = 2,6-Me_2-4-R''-C_6H_2 and R'' = H, Me, OMe or F) has a small, albeit detectable effect in the electronic properties of the cationic Rh(III) center and an also scant influence in the chemical reactivity.

EXPERIMENTAL SECTION

General Considerations. All operations were performed under an argon atmosphere using standard Schlenk techniques, employing dry solvents and glassware. Microanalyses were performed by the Microanalytical Service of the Instituto de Investigaciones Químicas (Sevilla, Spain. The NMR instruments were Bruker DRX–500, DRX–400 and DRX–300 spectrometers. Spectra were referenced to external $SiMe_4$ (δ 0 ppm) using the residual proton solvent peaks as internal standards (^{1}H NMR experiments), or the characteristic resonances of the solvent nuclei (^{13}C NMR experiments), while $^{31}P\{^1H\}$ NMR spectra were referenced to external H_3PO_4. Spectral assignments were made by routine one- and two-dimensional NMR experiments where appropriate. Metal complexes $Zn(\eta^5\text{-}C_5Me_5)_2$, $Zn(C_5Me_4{}^tBu)_2$, $Zn[C_5Me_4(3,5\text{-}{}^tBu_2C_6H_3)]_2$, $[RhCl(C_2H_4)]_2$, as well as $NaBAr_F$ (BAr_F = $B[(C_6H_3\text{-}3,5\text{-}(CF_3)_2)_4]$)[28] and the phosphines of the type $PMe(Xyl')_2$ and $PEt(Xyl)_2$ were prepared according to literature procedures.[11]

Synthesis and characterization of complex 1a. A solution of the corresponding phosphine (0.5 mmol) in 3 mL of THF was added, at -40 ºC, to a solution of $[RhCl(C_2H_4)_2]_2$ (0.25 mmol) in 3 mL of THF. The reaction mixture was stirred for 3 h at this temperature. Then, a solution of $Zn(\eta^5\text{-}C_5Me_5)_2$ (0.25 mmol) in 2 mL of THF was added and the mixture stirred for 5 h at -25 ºC. At this temperature the solvent was removed under vacuum, the residue extracted with diethyl ether and the resulting solution evaporated to dryness. The dark yellow solid obtained contains a mixture of complexes **1a** and **2a**. To the solid mixture was added a $NaBH_4$ (0.26 mmol) solution in ethanol:THF (3:1 mixture, 5 mL) and stirred at room temperature for 10 minutes. Analytically pure samples of complex **1a** could not be obtained. Thus, characterization of **1a** was carried out in solution by NMR spectroscopy of the reaction crude. ^{1}H RMN (400 MHz, C_6D_6, 25 ºC) δ: 7.45 (d, 1 H, H_a), 7.06 (td, 1 H, $^5J_{HP}$ = 2.8 Hz, H_b), 6.94 (td, 1 H, $^5J_{HP}$ = 1.6 Hz, H_e), 6.84, 6.73, 6.71 (m, 1 H each, H_d, H_f, H_c), 3.59 (d, 1 H, $^2J_{HH}$ = 13.6, RhC*H*H), 3.00 (dd, 1 H, $^2J_{HRh}$ = 4.2 Hz, RhCH*H*), 2.36, 1.63 (s, 3 H each, Me_β, Me_γ), 1.93 (d, 3 H, $^2J_{HP}$ = 9.0 Hz, PMe), 1.89 (s, 3 H, Me_α), 1.69 (d, 15 H, $^4J_{HP}$ = 1.6 Hz, C_5Me_5), -13.77 (dd, 1 H, $^1J_{RhH}$ = 46.0, $^2J_{HP}$ = 37.0 Hz, RhH). All aromatic $^3J_{HH}$ couplings were *ca.* 7.5 Hz. $^{13}C\{^1H\}$ RMN (100 MHz, C_6D_6, 25 ºC) δ: 158.6 (d, $^2J_{CP}$ = 33 Hz, C_1), 141.9 (dd, $^1J_{CP}$ = 54, $^2J_{CRh}$ = 4 Hz, C_2), 141.9, 139.0 (d, $^2J_{CP}$ = 8 Hz, C_4, C_6), 138.8 (C_3), 134.0 (d, $^1J_{CP}$ = 27 Hz, C_5), 129.9, 129.8 (d, $^3J_{CP}$ = 7 Hz, CH_d, CH_f), 129.2 (CH_b), 128.7 (CH_e), 127.3 (d, $^3J_{CP}$ = 16 Hz, CH_a), 127.1 (d, $^3J_{CP}$ = 7 Hz, CH_c), 96.9 (dd, $^1J_{CRh}$ = $^2J_{CP}$ = 3 Hz, *C*$_5$Me$_5$), 21.7 (d, $^1J_{CP}$ = 38 Hz, PMe), 25.4, 22.4 (d, $^3J_{CP}$ = 4, $^3J_{CP}$ = 9 Hz, Me_β, Me_γ), 22.4 (dd, $^1J_{CRh}$ = 26, $^2J_{CP}$ = 4 Hz, $RhCH_2$), 20.9 (d, $^3J_{CP}$ = 3 Hz, Me_α), 10.6 (C_5Me_5). $^{31}P\{^1H\}$ RMN (160 MHz, C_6D_6, 25 ºC) δ: 49.9 (d, $^1J_{PRh}$ = 156 Hz).

Synthesis of complexes 2. A solution of the corresponding phosphine (0.5 mmol) in 2 mL of THF was added, at -40 ºC, to a solution of $[RhCl(C_2H_4)_2]_2$ (0.25 mmol) in 3 mL of THF. The reaction mixture was stirred for 3 h at this temperature. Then, a solution of the corresponding $Zn(\eta^5\text{-}C_5Me_4R)_2$ (0.25 mmol) in 1 mL of THF was added and the mixture stirred for 5 h at -25 ºC. After warming up at room temperature the solvent was removed under vacuum and the residue extracted with diethyl ether and the

resulting solution evaporated to dryness. The solid obtained was dissolved in 5 mL of $CHCl_3$ and stirred for 3 h at room temperature. The solvent was removed under vacuum and the crude product washed with pentane to yield complexes **2a-2g** as red/orange solids in 70-80%. These complexes can be recrystallized from diethyl ether. **Complex 2b**. Anal. Calc. for $C_{29}H_{39}ClPRh$: C, 62.5; H, 7.1. Found: C, 62.7; H, 6.9. ^{1}H NMR (500 MHz, 25 ºC, $CDCl_3$) δ: 7.07 (s, 1 H, H_a), 6.93 (s, 1 H, $H_{c/d}$), 6.70 (s, 1 H, $H_{d/c}$), 6.63 (s, 1 H, H_b), 3.53 (dt, 1 H, $^2J_{HH}$ = 12.9, $^2J_{HRh}$ = $^3J_{HP}$ = 3.0 Hz, RhC*H*H), 3.40 (dd, 1 H, $^2J_{HH}$ = 12.9, $^3J_{HRh}$ = 2.5 Hz, RhCH*H*), 2.56 (s, 3 H, $Me_{\gamma/\varepsilon}$), 2.26 (s, 3 H, Me_δ), 2.56 (s, 3 H, Me_β), 2.17 (d, 3 H, $^2J_{HP}$ = 10.4 Hz, PMe), 1.92 (s, 3 H, Me_α), 1.47 (s, 3 H, $Me_{\varepsilon/\gamma}$), 1.41 (d, 15 H, $^4J_{HP}$ = 2.3 Hz, C_5Me_5). ^{13}C{^{1}H} NMR (125 MHz, 25 ºC, $CDCl_3$) δ: 157.0 (d, $^2J_{CP}$ = 33 Hz, C_1), 142.0 (d, $^2J_{CP}$ = 9 Hz, $C_{6/8}$), 140.0 (d, $^2J_{CP}$ = 8 Hz, $C_{6/8}$), 139.6, 139.4 (d, $^4J_{CP}$ = 2 Hz, C_4, C_7), 138.9 (C_3), 135.6 (dd, $^1J_{CP}$ = 55, $^2J_{CRh}$ = 2 Hz, C_2), 131.1, 130.8 (d, $^3J_{CP}$ = 8 Hz, CH_c, CH_d), 128.8 (d, $^3J_{CP}$ = 7 Hz, CH_b), 128.7 (d, $^1J_{CP}$ = 34 Hz, C_5), 127.7 (d, $^3J_{CP}$ = 17 Hz, CH_a), 98.2 (t, $^1J_{CRh}$ = $^2J_{CP}$ = 4 Hz, *C*$_5$Me$_5$), 34.2 (dd, $^1J_{CRh}$ = 24, $^2J_{CP}$ = 7 Hz, $RhCH_2$), 25.9 (d, $^3J_{CP}$ = 5 Hz, $Me_{\gamma/\varepsilon}$), 23.6 (d, $^3J_{CP}$ = 8 Hz, $Me_{\gamma/\varepsilon}$), 21.2, 21.1 (Me_β, Me_δ), 20.6 (d, $^3J_{CP}$ = 3 Hz, Me_α), 19.9 (d, $^1J_{CP}$ = 34 Hz, PMe), 8.8 (C_5*Me*$_5$). ^{31}P{^{1}H} NMR (200 MHz, 25 ºC, $CDCl_3$) δ: 44.1 (d, $^1J_{PRh}$ = 157 Hz).

Synthesis of complexes 3·CO$^+$. To a solid mixture of complexes **2a-2f** (0.08 mmol) and NaBArF (0.08 mmol), placed in a thick-wall ampoule, was added 5 mL of CH_2Cl_2 and the reaction mixture stirred for 10 min at room temperature under 1.5 bar of CO. After filtering, the solvent was evaporated under reduced pressure to obtain orange (**3c·CO$^+$**) and yellow powders (**3a·CO$^+$**, **3b·CO$^+$**, **3d·CO$^+$**, **3e·CO$^+$**, **3f·CO$^+$**) in ca. 95% yield. These complexes can be recrystallized by slow diffusion at -20 ºC of pentane into a CH_2Cl_2 solution (2:1 by vol.). **Complex 3b·CO$^+$**. IR (Nujol): 2050 cm^{-1}. Anal. Calc. for $C_{62}H_{51}BF_{24}OPRh$: C, 52.7; H, 3.6. Found: C, 52.5; H, 3.7. ^{1}H NMR (400 MHz, 25 ºC, CD_2Cl_2) δ: 7.20 (s, 1 H, H_a), 7.13 (s, 1 H, $H_{c/d}$), 6.94 (s, 2 H, $H_{d/c}$, H_b), 3.53 (dd, 1 H, $^2J_{HH}$ = 12.5, $^2J_{HRh}$ = 2.0 Hz, RhC*H*H), 3.32 (dd, 1 H, $^2J_{HH}$ = 12.5, $^2J_{HRh}$ = 4.2 Hz, RhCH*H*), 2.52 (s, 3 H, $Me_{\gamma/\varepsilon}$), 2.37 (s, 3 H, $Me_{\beta/\delta}$), 2.36 (d, 3 H, $^2J_{HP}$ = 9.7 Hz, PMe), 2.35 (s, 3 H, $Me_{\delta/\beta}$), 2.04 (s, 3 H, Me_α), 1.71 (d, 15 H, $^4J_{HP}$ = 2.8 Hz, C_5Me_5), 1.53 (s, 3 H, $Me_{\varepsilon/\gamma}$). ^{13}C{^{1}H} NMR (100 MHz, 25 ºC, CD_2Cl_2) δ: 188.7 (dd, $^1J_{CRh}$ = 73, $^2J_{CP}$ = 19 Hz, CO), 152.1 (d, $^2J_{CP}$ = 29 Hz, C_1), 142.8, 142.6 (d, $^4J_{CP}$ = 3 Hz, C_4, C_7), 142.1 (d, $^1J_{CP}$ = 10 Hz, $C_{6/8}$), 140.3 (d, $^2J_{CP}$ = 8 Hz, $C_{8/6}$), 139.8 (t, $^2J_{CP}$ = $^3J_{CRh}$ = 3 Hz, C_3), 132.6 (dd, $^1J_{CP}$ = 61, $^2J_{CRh}$ = 3 Hz, C_2), 131.8, 131.6 (d, $^3J_{CP}$ = 9 Hz, CH_c, CH_d), 130.8 (d, $^3J_{CP}$ = 8 Hz, CH_b), 126.8 (dd, $^3J_{CP}$ = 17, $^3J_{CRh}$ = 2 Hz, CH_a), 121.8 (d, $^1J_{CP}$ = 42 Hz, C_5), 106.1 (dd, $^1J_{CRh}$ = 4, $^2J_{CP}$ = 2 Hz, *C*$_5$Me$_5$), 28.4 (d, $^1J_{CRh}$ = 21 Hz, $RhCH_2$), 25.5 (d, $^3J_{CP}$ = 6 Hz, $Me_{\gamma/\varepsilon}$), 25.2 (d, $^1J_{CP}$ = 40 Hz, PMe), 23.2 (d, $^3J_{CP}$ = 8 Hz, $Me_{\varepsilon/\gamma}$), 20.6 (Me_β, Me_δ), 20.1 (d, $^3J_{CP}$ = 4 Hz, Me_α), 8.6 (C_5*Me*$_5$). ^{31}P{^{1}H} NMR (160 MHz, 25 ºC, CD_2Cl_2) δ: 36.1 (d, $^1J_{PRh}$ = 126 Hz).

Synthesis of complexes 3$^+$. To a mixture of **2a-2f** (0.15 mmol) and NaBArF (0.15 mmol) was added 5 mL of CH_2Cl_2 under argon. The reaction mixture was stirred for 10 min at room temperature, after which the solution turned from orange to red. The resulting suspension was filtered and the solvent evaporated under reduced pressure to obtain compounds **3a$^+$-3f$^+$** as red solids in ca. 95% yield. For further purification, the complexes can be recrystallized by slow diffusion at -20 ºC of pentane into a CH_2Cl_2 solution (2:1 by vol.). **Complex 3b$^+$.** Anal. Calc. for C61H51BF24PRh: C, 52.9; H, 3.7. Found: C, 52.6; H, 3.7. ^{1}H NMR (400 MHz, 25 ºC, $CDCl_3$) δ: 7.34 (s, 1 H, H_b), 6.88, 6.76 (s, 1 H, $H_{c/d}$), 6.60 (s, 1 H, H_a), 2.91 (dt, 1 H, $^2J_{HH}$ = 4.0, $^2J_{HRh}$ = $^3J_{HP}$ = 1.3 Hz, $RhCH_\alpha$), 2.51 (s, 3 H, $Me_{\gamma/\varepsilon}$), 2.44 (s, 3 H, Me_α), 2.36 (s, 3 H, Me_β), 2.20 (s, 3 H, Me_δ), 2.11 (d, 3 H, $^2J_{HP}$ = 13.0 Hz, PMe), 1.97 (s, 3 H, $Me_{\varepsilon/\gamma}$), 1.61 (d, 15 H, $^4J_{HP}$ = 2.7 Hz, C_5Me_5), 1.29 (ddd, 1 H, $^3J_{HP}$ = 13.9, $^2J_{HH}$ = 4.0, $^2J_{HRh}$ = 0.7 Hz, $RhCH_\beta$). ^{13}C{^{1}H} NMR (100 MHz, 25 ºC, $CDCl_3$) δ: 144.1 (C_4), 143.2 (C_8), 141.9, 140.9 (C_5, C_7), 137.3 (C_3), 134.7 (CH_b), 130.4, 130.3 (CH_c, CH_d), 125.1 (d, $^3J_{CP}$ = 8 Hz, CH_a), 116.7 (d, $^1J_{CP}$ = 58 Hz, C_6), 104.6 (dd, $^1J_{CRh}$ = 14, $^2J_{CP}$ = 4 Hz, C_1), 98.8 (dd, $^1J_{CRh}$ = 6, $^2J_{CP}$ = 2 Hz, *C*$_5$Me$_5$), 74.4 (d, $^1J_{CP}$ = 25 Hz, C_2),

41.5 (dd, $^2J_{CP}$ = 15, $^1J_{CRh}$ = 2 Hz, $RhCH_2$), 22.5 (Me_α), 21.7, 21.5 ($Me_{\gamma/\varepsilon}$), 21.1 (Me_β), 20.9 (Me_δ), 13.0 (d, $^1J_{CP}$ = 33 Hz, PMe), 8.9 (C_5Me_5). $^{31}P\{^1H\}$ NMR (160 MHz, 25 ºC, $CDCl_3$) δ: - 15.7 (d, $^1J_{PRh}$ = 138 Hz).

X-Ray Structure Analysis of Complexes 2a, 2b, 2g, 3a$^+$, 3d$^+$, 3e$^+$ and 3f$^+$. A summary of the crystallographic data and structure refinement of these new crystalline compounds is given at the Supporting Information. A single crystal of suitable size, coated with dry perfluoropolyether (Fomblin Y H-VAC 140/13), was mounted on a glass fiber and fixed in a cold nitrogen stream (T = 100(2) K) to the goniometer head. Data collection was performed on Bruker-Nonius X8APEX-II CCD diffractometer, using monochromatic radiation λ(Mo $K_{\alpha1}$) = 0.71073 Å, by means of ω and φ scans with a width of 0.5º. The data were reduced (SAINT)[30] and corrected for Lorentz polarization effects and absorption by multiscan method applied by SADABS.[31] The structures were solved by direct methods (SIR-2002)[32] and refined against all F^2 data by full-matrix least-squares techniques (SHELXTL-6.12).[33] All the non-hydrogen atoms were refined with anisotropic displacement parameters. The hydrogen atoms were included from calculated positions and refined riding on their respective carbon atoms with isotropic displacement parameters.

COMPUTATIONAL DETAILS

Geometry optimizations were carried out at the DFT level with Gaussian 09[29] using the meta-GGA functional M06.[30] The C, H and P atoms were described with the 6-31G(d,p) basis set[31] and the Rh atoms were represented by the Stuttgart/Dresden Effective Core Potential and the associated basis set (SDD).[32] Optimizations were made in the gas phase without restrictions. The stationary points of the Potential Energy Surface and their nature as minima or saddle points (TS) were characterized by vibrational analysis, which also gave gas-phase enthalpies (H), entropies (S) and Gibbs energies (G). The minima connected by a given transition state were determined by Intrinsic Reaction Coordinate (IRC) calculations or by perturbing the transition states along the TS coordinate and optimizing to the nearest minimum. The solvent effects (dichloromethane) were modelled with the SMD continuum model by single point calculations on gas phase-optimized geometries.[33] Atoms In Molecules analysis of the electron density was performed with the Multiwfn program[34] on wave functions calculated for species reoptimized at the DFT, M06, 6-311g(d,p)[35] + SDD level. The same level of theory was used to construct the natural bonding orbitals, which were analyzed with the NBO6.0 suite.[36]

ASSOCIATED CONTENT

Supporting Information

Analytical and spectroscopic data for complexes **1·SiMe$_3$**, **2c-g**, **3a·C$_2$H$_4^+$**, **3a·CNXyl$^+$**, **3a·NH$_3^+$**, **3a·PMe$_3^+$**, **3c$^+$-3f$^+$**; $^{13}C\{^1H\}$ and ^{13}C NMR spectrum of **3a$^+$**; low temperature reaction of **3$^+$** with H_2; Spectroscopic data of agostic hydrides **4$^+$**; general procedure for Si–H/Si–D exchanges; general method for the hydrosilylation of C-O multiple bonds; kinetic studies; X-Ray structure analysis of **2a**, **2b**, **2g**, **3a$^+$**, **3d$^+$**, **3e$^+$**, **3f$^+$**, **3a·CO$^+$**, **3a·NCCH$_3^+$** and **3a·C$_2$H$_4^+$**; additional figures and tables with computational details.

This material is available free of charge via the Internet at http://pubs.acs.org

AUTHOR INFORMATION

Corresponding Author

*E. C.: e-mail, guzman@us.es; fax, (+34)95-446-0165

Notes

The authors declare no competing financial interests.

ACKNOWLEDGMENT

Financial support (FEDER support) from the Spanish Ministerio de Ciencia e Innovación (Project No. CTQ2013-42501-P) is gratefully acknowledged. The use of computational facilities of the supercomputing center of Galicia, CESGA, and of the Centro de Servicios de Informática y Redes de Comunicaciones (CSIRC) of the Universidad de Granada (UGR) is also acknowledged. M. F. E. thanks the Universidad de Sevilla for a research grant.

REFERENCES

(1) (a) G. Song, F. Wang, X. Li, *Chem. Soc. Rev.* **2012**, *41*, 3651-3678; (b) M. Albrecht, *Chem. Rev.* **2010**, *110*, 576–623; (c) S. Kuwata, T. Ikariya, *Dalton Trans.* **2010**, *39*, 2984–2992; (d) Z. Liu, P. J. Sadler, *Acc. Chem. Res.* **2014**, *47*, 1174-1185; (e) R. G. Bergman, *Nature* **2007**, *446*, 391-393.

(2) (a) L. S. Sharninghausen, J. Campos, M. G. Manas, R. H. Crabtree, *Nat. Commun.* **2014**, *5*, 5084; (b) O. Díaz-Morales, T. J. P. Hersbach, D. G. H. Hetterscheid, J. N. H. Reek, M. T. M. Koper, *J. Am. Chem. Soc.* **2014**, *136*, 10432-10439; (c) E. Kumaran, W. K. Leong, *Organometallics* **2012**, *31*, 4849-4853; (d) C. Wang, B. Villa-Marcosa, J. Xiao, *Chem. Commun.* **2011**, *47*, 9773–9785.

(3) (a) A. J. Cheney, B. E. Mann, B. L. Shaw, R. M. Slad, *J. Chem. Soc. D* **1970**, 1176-1177; (b) A. J. Cheney, B. E. Mann, B. L. Shaw, R. M. Slade, *J. Chem. Soc. A* **1971**, 3833-3842; (c) A. J. Cheney, B. L. Shaw, *J. Chem. Soc., Dalton Trans.* **1972**, 754-763.

(4) J. Campos, A. C. Esqueda, J. López-Serrano, L. Sánchez, F. P. Cossio, A. de Cozar, E. Álvarez, C. Maya, E. Carmona, *J. Am. Chem. Soc.* **2010**, *132*, 16765–16767.

(5) (a) J. Campos, J. Lopez-Serrano, E. Alvarez, E. Carmona, *J. Am. Chem. Soc.* **2012**, *134*, 7165-7175; (b) J. Campos, E. Álvarez, E. Carmona, *New J. Chem.* **2011**, *35*, 2122; (c) J. Campos, A. C. Esqueda, E. Carmona, *Chem. Eur. J.* **2010**, *16*, 419-422.

(6) J. Campos, M. F. Espada, J. Lopez-Serrano, E. Carmona, *Inorg. Chem.* **2013**, *52*, 6694-6704.

(7) J. Campos, E. Carmona, *Organometallics* **2015**, *34*, 2212–2221.

(8) (a) P. Burger, R. G. Bergman, *J. Am. Chem. Soc.* **1993**, *115*, 10462-10463; (b) F. L. Taw, H. Mellows, P. S. White, F. J. Hollander, R. G. Bergman, M. Brookhart, D. M. Heinekey, *J. Am. Chem. Soc.* **2002**, *124*, 5100-5108.

(9) O. K. Cambridge Structural Database (Version 5.36); F. H. Allen, *Chem. Des. Automat. News* **1993**, *8*, 31 – 37.

(10) (a) M. Rubio, J. Campos, E. Carmona, *Org. Lett.* **2011**, *13*, 5236–5239; (b) J. Campos, M. Rubio, A. C. Esqueda, E. Carmona, *J. Labelled Compd. Radiopharm*. **2012**, *55*, 29-38.

(11) A. C. Esqueda, S. Conejero, C. Maya, E. Carmona, *Organometallics* **2010**, *29*, 5481-5489.

(12) (a) D. F. Shriver, *Acc. Chem Res.* **1970**, *3*, 231-238; b) R. J. Angelici, *Acc. Chem. Res.* **1995**, *28*, 51-60.

(13) A. S. Goldman, K. Krogh-Jespersen, *J. Am. Chem. Soc.* **1996**, *118*, 12159–12166.

(14) D. Buchholz, L. Zsolnai, G. Huttner, D. Astruc, *J. Organomet. Chem.* **2000**, 593-594, 494–496.

(15) (a) M. Brookhart, M. L. H. Green, *J. Organomet. Chem.* **1983**, *250*, 395-408; (b) M. Brookhart, M. L. H. Green, G. Parkin, *Proc. Natl. Acad. Sci. U. S. A.* **2007**, *104*, 6908-6914; (c) J. C. Green, M. L. H. Green, G. Parkin, *Chem. Commun.* **2012**, *48*, 11481-11503.

(16) R. F. W. Bader, Atoms in Molecules: A Quantum Theory, Oxford University Press: Oxford, UK, **1995**.

(17) (a) P. R. Varadwaj, A. Varadwaj, H. M. Marques, *J. Phys. Chem. A* **2011**, *115*, 5592-5601; (b) P. R. Varadwaj, I. Cukrowski, H. M. Marques, *J. Phys. Chem. A* **2008**, *112*, 10657-10666.

(18) F. Weinhold, *J. Comput. Chem.* **2012**, *33*, 2363–2379.
(19) (a) M. J. Fernandez, P. M. Bailey, P. O. Bentz, J. S. Ricci, T. F. Koetzle, P. M. Maitlis, *J. Am. Chem. Soc.* **1984**, *106*, 5458–5463; (b) S. B. Duckett, D. M. Haddleton, S. A. Jackson, R. N. Perutz, M. Poliakoff, R. K. Upmacis, *Organometallics* **1988**, *7*, 1526–1532.
(20) S. B. Sinha, D. Y. Shopov, L. S. Sharninghausen, D. J. Vinyard, B. Q. Mercado, G. W. Brudvig, R. H. Crabtree, *J. Am. Chem. Soc.* **2015**, *137*, 15692-15695.
(21) (a) R. H. Crabtree, *Angew. Chem. Int. Ed.* **1993**, *32*, 789–805; (b) G. J. Kubas, Metal Dihydrogen and Sigma-Bond Complexes. Structure Theory and Reactivity, Kluwer Academic, New York, **2001**.
(22) J. Yang, P. S. White, C. K. Schauer, M. Brookhart, *Angew. Chem. Int. Ed.* **2008**, *47*, 4141-4143.
(23) (a) B. Marciniec, *Silicon Chemistry* **2002**, *1*, 155-174; (b) A. K. Roy, *Adv. Organomet. Chem.* **2007**, *55*, 1-59; (c) R. Malacea, R. Poli, E. Manoury, *Coord. Chem. Rev.* **2010**, *254*, 729-752; (d) R. H. Morris, *Chem. Soc. Rev.* **2009**, *38*, 2282-2291; (e) B. Marciniec, Comprehensive Handbook on Hydrosilylation, Pergamon, Oxford, **1992**.
(24) (a) E. Calimano, T. D. Tilley, *J. Am. Chem. Soc.* **2009**, *131*, 11161-11173; (b) S. Park, M. Brookhart, *Organometallics* **2010**, *29*, 6057-6064; (c) J. Yang, P. S. White, M. Brookhart, *J. Am. Chem. Soc.* **2008**, *130*, 17509-17518; (d) A. M. Tondreau, E. Lobkovsky, P. J. Chirik, *Org. Lett.* **2008**, *10*, 2789-2792; (e) A. M. Tondreau, C. C. H. Atienza, K. J. Weller, S. A. Nye, K. M. Lewis, J. G. P. Delis, P. J. Chirik, *Science* **2012**, *335*, 567-570; (f) J. Yang, T. D. Tilley, *Angew. Chem. Int. Ed.* **2010**, *49*, 10186-10188; (g) J. M. Blackwell, D. J. Morrison, W. E. Piers, *Tetrahedron* **2002**, *58*, 8247–8254; (h) Z. A. Buchan, S. J. Bader, J. Montgomery, *Angew. Chem. Int. Ed.* **2009**, *48*, 4840-4844; (i) B. L. Tran, M. Pink, D. J. Mindiola, *Organometallics* **2009**, *28*, 2234–2243.
(25) (a) D. J. Parks, W. E. Piers, *J. Am. Chem. Soc.* **1996**, *118*, 9440-9441; (b) D. J. Parks, W. E. Piers, M. Parvez, R. Atencio, M. J. Zaworotko, *Organometallics* **1998**, *17*, 1369-1377; (c) D. J. Parks, J. M. Blackwell, W. E. Piers, *J. Org. Chem.* **2000**, *65*, 3090-3098.
(26) (a) I. Ojima, T. Kogure, M. Kumagai, S. Horiuchi, T. Sato, *J. Organomet. Chem.* **1976**, *122*, 83-97; (b) S. B. Duckett, R. N. Perutz, *Organometallics* **1992**, *11*, 90-98.
(27) R. N. Perutz, S. Sabo-Etienne, *Angew. Chem. Int. Ed.* **2007**, *46*, 2578-2592.
(28) (a) N. A. Yakelis, R. G. Bergman, *Organometallics* **2005**, *24*, 3579-3581; (b) R. Bloom, J. Boersma, P. H. M. Budzelaar, B. Fischer, A. Haaland, H. V. Volden, J. Weidlein, *Acta Chem. Scand.* **1986**, *40*, 113-120; (c) G. Giordano, R. H. Crabtree, *Inorg. Synth.* **1979**, *19*, 218-220; (d) R. Cramer, *Inorg. Synth.* **1974**, *14*, 15.
(29) Gaussian 09, Revision E.01, M. J. Frisch, G. W. Trucks, H. B. Schlegel, G. E. Scuseria, M. A. Robb, J. R. Cheeseman, G. Scalmani, V. Barone, B. Mennucci, G. A. Petersson, H. Nakatsuji, M. Caricato, X. Li, H. P. Hratchian, A. F. Iz-maylov, J. Bloino, G. Zheng, J. L. Sonnenberg, M. Hada, M. Ehara, K. Toyota, R. Fukuda, J. Hasegawa, M. Ishida, T. Nakajima, Y. Honda, O. Kitao, H. Nakai, T. Vreven, J. A. Montgomery, Jr., J. E. Peralta, F. Ogliaro, M. Bearpark, J. J. Heyd, E. Brothers, K. N. Kudin, V. N. Staroverov, T. Keith, R. Kobayashi, J. Normand, K. Raghavachari, A. Rendell, J. C. Burant, S. S. Iyengar, J. Tomasi, M. Cossi, N. Rega, J. M. Millam, M. Klene, J. E. Knox, J. B. Cross, V. Bakken, C. Adamo, J. Jaramillo, R. Gomperts, R. E. Stratmann, O. Yazyev, A. J. Austin, R. Cammi, C. Pomelli, J. W. Ochterski, R. L. Martin, K. Morokuma, V. G. Zakrzewski, G. A. Voth, P. Salvador, J. J. Dannenberg, S. Dapprich, A. D. Daniels, O. Farkas, J. B. Foresman, J. V. Ortiz, J. Cioslowski, D. J. Fox, Gaussian, Inc., Wallingford CT, **2013**.
(30) Y. Zhao, D. Truhlar, *Theor. Chem. Acc.* **2008**, *120*, 215-241.
(31) (a) W. J. Hehre, R. Ditchfield, J. A. Pople, *J. Phys. Chem.* **1972**, *56*, 2257; (b) P. C. Hariharan, J. A. Pople, *Theor. Chim. Acta.* **1973**, *28*, 213; (c) M. M. Francl, W. J. Pietro, W. J. Hehre, J. S. Binkley, M. S. Gordon, D. J. Defrees, J. A. Pople, *J. Chem. Phys.* **1982**, *77*, 3654.
(32) D. Andrae, U. H., M. Dolg, H. Stoll, H. Preul, *Theor. Chem. Acc.* **1990**, 123-141.
(33) A. V. Marenich, C. J. Cramer, D. G. Truhlar, *J. Phys. Chem. B* **2009**, *113*, 6378-6396.

(34) T. Lu, F. W. Chen, *J. Comput. Chem.* **2012**, *33*, 580−592
(35) (a) A. D. McLean, G. S. Chandler, *J. Chem. Phys.* **1980**, *72*, 5639-5648; (b) K. Raghavachari, J. S. Binkley, R. Seeger, J. A. Pople, *J. Chem. Phys.* **1980**, *72*, 650-654.
(36) NBO 6.0. E. D. Glendening, J, K. Badenhoop, A. E. Reed, J. E. Carpenter, J. A. Bohmann, C. M. Morales, C. R. Lan-dis, and F. Weinhold, Theoretical Chemistry Institute, University of Wisconsin, Madison, **2013**.